Mon. Not. R. Astron. Soc. **264**, 1018–1024 (1993)

A new strategy for 2D inversion for solar rotation

Takashi Sekii

Institute of Astronomy, Madingley Road, Cambridge CB3 0HA

Accepted 1993 May 21. Received 1993 May 20; in original form 1993 March 31

ABSTRACT

In the linearized integral formula for rotational splitting of solar p-mode frequencies, the dominant term in the kernel is a product of two terms, one depending on the radial coordinate alone, and the other depending solely on the colatitude. By retaining only this term in the equation, two-dimensional inverse techniques for the solar internal rotation can be formulated in such a way that the angular and radial inversions can be carried out separately. Thus the 2D inversion is reduced to two successive 1D inversions. This strategy leads to a dramatic reduction in computational burden when one is inverting huge data sets. It is also possible to improve the quality of the inversions significantly by a modification to the radial inversion procedure. In this paper, regularized least-squares data fitting and a modified optimally localized averaging are applied to the angular inversion and the radial inversion, respectively. The quality of the inversions is illustrated by means of the resulting averaging kernels.

Key words: methods: data analysis – Sun: oscillations – Sun: rotation.

1 INTRODUCTION

Helioseismic inversion is a powerful tool for probing internal angular flow of the Sun. Under the influence of rotation, the degeneracy of the eigenfrequencies with respect to azimuthal order m is lifted. In the linear regime the shift of the eigenfrequency is a weighted average of angular velocity. Since different modes sample the angular velocity differently, one can attempt to infer the internal angular velocity of the Sun from precise measurement of the oscillation eigenfrequencies.

In the early days of helioseismology, observations were available only for sectoral modes (Duvall & Harvey 1984), which sample the angular velocity mainly near the equator. Accordingly, early inversions were carried out in one dimension, in which the angular velocity was considered to be averaged over latitudes in the vicinity of the equator (Duvall et al. 1984; Gough 1984). Owing to recent improvements in the quality of the data, one can now tackle 2D problems: one can infer the angular velocity Ω as a function of both the radial coordinate r and the colatitude θ (see, for example, Brown et al. 1989). Fully two-dimensional inversions have been discussed by Sekii (1990, 1991), Schou (1991) and Schou, Christensen-Dalsgaard & Thompson (1993a,b). For a recent review of the field in general, see Gough & Toomre (1991).

We are expecting in the near future huge data sets from the GONG project (Harvey et al. 1993) and from the Solar Oscillations Investigation on the spacecraft *SOHO* (Scherrer et al. 1989); frequency splittings will be obtained for each singlet, defined by its radial order n, its spherical harmonic degree l and its azimuthal order. The number of modes with different (nlm) is expected be of the order of 10^5. Efficient methods for handling such huge data sets are therefore necessary.

One possible strategy, which decreases the numerical effort dramatically, is to separate the angular inversion from the radial inversion, and carry them out successively (Sekii 1993). Here I discuss this strategy in the case when regularized least-squares data fitting is used for the angular inversions and optimally localized averaging is used for the radial inversions. Averaging kernels produced by these procedures are examined to evaluate the quality of the inversions. A slight modification to the radial inversion can improve the averaging kernels significantly.

2 TWO-DIMENSIONAL INVERSION OF ROTATIONAL SPLITTING

The linear formula for the frequency shift $\Delta\omega_{nlm}$ due to the angular velocity $\Omega(r,\theta)$ about the axis of spherical polar coordinates (r,θ,ϕ) is presented, for example, by Hansen, Cox & Van Horn (1977). The formula can be rewritten in the form

$$\frac{\Delta\omega_{nlm}}{m} = \int [F_{nl}(\mu)W_{lm}(\mu) + G_{nl}(\mu)X_{lm}(\mu)]\mathrm{d}\mu \ , \tag{2.1}$$

where $\Delta\omega_{nlm}$ is the antisymmetric part $\frac{1}{2}(\omega_{n,l,m} - \omega_{n,l,-m})$ of the frequency splitting, and

$$F_{nl}(\mu) = \int_0^R K_{nl}(r)\Omega(r,\mu)\rho r^2 \mathrm{d}r \ , \tag{2.2}$$

$$G_{nl}(\mu) = \int_0^R L_{nl}(r)\Omega(r,\mu)\rho r^2 \mathrm{d}r \ , \tag{2.3}$$

$$I_{nl} = \int_0^R [\xi_r^2 + l(l+1)\xi_h^2]\rho r^2 \mathrm{d}r \ , \tag{2.4}$$

$$K_{nl}(r) = [\xi_r^2 + l(l+1)\xi_h^2 - 2\xi_r\xi_h]\rho r^2/I_{nl} \ , \tag{2.5}$$

$$L_{nl}(r) = \xi_h^2 \rho r^2/I_{nl} \ , \tag{2.6}$$

$$W_{lm}(\mu) = P_l^m(\mu)^2 \ , \tag{2.7}$$

$$X_{lm}(\mu) = (1-\mu^2)\frac{\mathrm{d}}{\mathrm{d}\mu}\left[P_l^m(\mu)\frac{\mathrm{d}P_l^m(\mu)}{\mathrm{d}\mu}\right] \ ; \tag{2.8}$$

here, $\mu = \cos\theta$, ρ is density, and $\xi_r(r)$ and $\xi_h(r)$ are real amplitude functions associated with the radial and horizontal components of the displacement vector $\boldsymbol{\xi}_{nlm}$ of the mode (nlm):

$$\boldsymbol{\xi}_{nlm} = \Re\left[\left(\xi_r,\ \xi_h\frac{\partial}{\partial\theta},\ \frac{\xi_h}{\sin\theta}\frac{\partial}{\partial\phi}\right)P_l^m(\mu)\mathrm{e}^{\mathrm{i}(m\phi-\omega_{nlm}t)}\right] \ ,$$

and $P_l^m(\mu)$ is an associated Legendre function.

The most straightforward way of inferring $\Omega(r,\mu)$ is to try to satisfy all the constraints (2.1) at once. This is the usual procedure for the one-dimensional case, but it can become difficult when the number of modes becomes very large.

We note that L_{nl} is proportional to ξ_h^2, which in the case of solar *p*-mode oscillations of high order is small everywhere except near the lower turning point (e.g. Unno et al. 1989), and thus the term $G_{nl}X_{lm}$ can be neglected in the first approximation. The simplification that this introduces permits the following $\mathrm{R}^1 \otimes \mathrm{R}^1$ inversion procedure (Sekii 1993): first, the set of constraints

$$\frac{\Delta\omega_{nlm}}{m} = \int F_{nl}(\mu)W_{lm}(\mu)\mathrm{d}\mu \ , \ m = 1, ..., l \tag{2.9}$$

is inverted for $F_{nl}(\mu)$, and then equation (2.2) is inverted for $\Omega(r,\mu)$ using all relevant (nl). These two steps will be called the angular inversion and the radial inversion respectively.

In the angular inversion the number of equations is l. Although the computation is easier, it is difficult to obtain a reliable result from low-degree modes, which provide only a small number of constraints.

In the next section I discuss the averaging kernels produced by this method.

3 AVERAGING KERNELS FROM $\mathrm{R}^1 \otimes \mathrm{R}^1$ INVERSIONS

Generally, the outcome of an angular inversion can be expressed as a linear combination of the data: the estimate of $F_{nl}(\mu_0)$ is given by

$$\hat{F}_{nl}(\mu_0) = \sum_m \beta_{lm}(\mu_0)\frac{\Delta\omega_{nlm}}{m} \ , \tag{3.1}$$

where the β_{lm} are inversion coefficients for the target colatitude $\theta_0 = \cos^{-1}\mu_0$. (In general, the coefficients depend also on n, and should strictly be written as β_{nlm}. Here, however, I assume that they are independent of n. I return to this point in Section 5.) It is normally the desire to obtain an estimate $\hat{F}_{nl}(\mu_0)$ that is a well-localized average of $F_{nl}(\mu)$. Therefore the aim is to find coefficients β_{lm} such that

$$\sum_m \beta_{lm}(\mu_0)W_{lm}(\mu) \equiv W_l(\mu;\mu_0) \simeq \delta(\mu-\mu_0) \ . \tag{3.2}$$

The function $W_l(\mu;\mu_0)$ is the angular averaging kernel; it is normalized to have unit modulus.

Similarly, for a target position r_0, a radial inversion produces inversion coefficients $c_{nl}(r_0)$ for which

$$\sum_{nl} c_{nl}K_{nl}(r) \simeq \delta(r-r_0) \ . \tag{3.3}$$

These results are combined to estimate the angular velocity at the target point (r_0, μ_0) as follows:

$$\begin{aligned}\hat{\Omega}(r_0,\mu_0) &= \sum_{nl} c_{nl}\hat{F}_{nl} \\ &= \sum_{nlm} c_{nl}\beta_{lm}\int K_{nl}(r)W_{lm}(\mu)\Omega(r,\mu) \ .\end{aligned} \tag{3.4}$$

Therefore the averaging kernel of the complete inversion is given by

$$\begin{aligned}D(r,\mu;r_0,\mu_0) &= \sum_{nlm} c_{nl}\beta_{lm}K_{nl}(r)W_{lm}(\mu) \\ &= \sum_{nl} c_{nl}K_{nl}(r)W_l(\mu;\mu_0) \ .\end{aligned} \tag{3.5}$$

In the angular direction, this averaging kernel is as well localized as is W_l. In the radial direction, however, the result is equivalent to the replacement of c_{nl} with $\tilde{c}_{nl} = W_l(\mu;\mu_0)c_{nl}$ in equation (3.3). If $\tilde{c}_{nl}/c_{nl}$ were constant, $D(r,\mu;r_0,\mu_0)$ would be localized radially in the same manner as $\sum c_{nl}K_{nl}(r)$. This condition requires that $W_l(\mu;\mu_0)$ be independent of l. Otherwise the averaging kernel D is liable to deviate from a well-localized form, although the angular average of the kernel would be identical to the radial averaging kernel obtained by attempting to satisfy equation (3.3).

The kernel $W_l(\mu;\mu_0)$ would be independent of l if it were the case that the angular inversions are perfect, i.e. $W_l(\mu;\mu_0) = \delta(\mu-\mu_0)$. However, one cannot hope for that to be so. Moreover, it is not guaranteed that one can construct kernels $W_l(\mu;\mu_0)$, of any finite width, that are *strictly* independent of l. Whilst the $\mathrm{R}^1 \otimes \mathrm{R}^1$ algorithm can produce a reasonable estimate of the angular velocity when $\Omega(r,\mu)$ is a smooth function (Sekii 1993), the potential distortion of the averaging kernel implies that this is not guaranteed in general. Moreover, one might expect that the distortion becomes increasingly serious as higher radial resolution is sought (leading to larger amplitudes of c_{nl}).

4 MODIFIED RADIAL INVERSION

Undesirable distortion of the averaging kernels resulting from imperfect angular inversions and a consequent l-dependence of the angular averaging kernel can be reduced by modifying the radial inversion procedure in the following manner. Instead of trying to satisfy equation (3.3), one chooses c_{nl} to localize

$$\begin{aligned}D(r,\mu;r_0,\mu_0) &= \sum_{nl} c_{nl}K_{nl}(r)\sum_m \beta_{lm}W_{lm}(\mu) \\ &= \sum_{nl} c_{nl}K_{nl}(r)W_l(\mu;\mu_0)\end{aligned} \tag{4.1}$$

in the radial direction. This can be accomplished by minimizing

$$\begin{aligned}S \equiv \int & \mathrm{d}r\mathrm{d}\mu D(r,\mu;r_0,\mu_0)^2(r-r_0)^2 \\ & + \alpha\sum_{nlm} c_{nl}^2\beta_{lm}^2 e_{nlm}^2\end{aligned} \tag{4.2}$$

subject to

$$\int \mathrm{d}r\mathrm{d}\mu D(r,\mu;r_0,\mu_0) = 1 \ ,$$

where the covariance matrix of the estimated errors $\sigma(\Delta\omega_{nlm})$ has been assumed to be of the form

$$m^{-2}\langle\sigma(\Delta\omega_{nlm})\sigma(\Delta\omega_{n'l'm'})\rangle = \delta_{nn'}\delta_{ll'}\delta_{mm'}e^2_{nlm} \ ,$$

and α is a regularization parameter. The numerical procedure is similar to the standard optimally localized averaging (e.g. Backus & Gilbert 1968, 1970; Gough 1985). Indeed, in the limit $W_l(\mu;\mu_0) \to \delta(\mu-\mu_0)$, the formulation is identical to the standard optimally localized averaging.

The complete procedure is therefore as follows:

(i) carry out the angular inversion to obtain β_{lm} and hence W_l;

(ii) apply the modified optimal averaging in the radial direction to obtain c_{nl}; and

(iii) combine c_{nl} and β_{lm} to estimate the angular velocity at the target point:

$$\hat{\Omega}(r_0,\mu_0) = \sum_{nl} c_{nl} \sum_{m} \beta_{lm} \frac{\Delta\omega_{nlm}}{m} \ .$$

The errors can also be estimated from these coefficients.

Note that now the coefficients c_{nl} depend also on μ_0, and thus should be written as $c_{nl}(r_0,\mu_0)$; the radial inversion must be carried out for each target colatitude. This was not necessary for the simplest form of $\mathrm{R}^1 \otimes \mathrm{R}^1$, although in practice one would do likewise in that case too, because the error property of $F_{nl}(\mu_0)$ depends on μ_0.

5 ANGULAR INVERSIONS

Angular inversions have been carried out using a least-squares data-fitting procedure. In this procedure one minimizes (Phillips 1962; Twomey 1963; Tikhonov1963)

$$\frac{1}{l}\sum_{m=1}^{l}\frac{1}{e^2_{nlm}}\left(\int_0^1 W_{lm}(\mu)F_{nl}(\mu)\mathrm{d}\mu - \frac{\Delta\omega_{nlm}}{m}\right)^2 + \lambda\int_0^1 |\mathscr{L}F_{nl}(\mu)|^2\mathrm{d}\mu \ , \tag{5.1}$$

where λ is a regularization parameter and $\mathscr{L}$ is a differential operator. The cases illustrated in this paper adopt the first derivative for $\mathscr{L}$. With the factor $1/l$, the first term is identical to χ^2. This scaling turns out to give a reasonably weak l-dependence of W_l (see Section 7).

The angular domain $0 \le \mu \le 1$ was divided into 100 intervals, and F_{nl} was represented by a continuous piecewise linear function. In the analysis of artificial data described below, the e_{nlm} were averaged over n, and this value was used in the expression (5.1); in this way, inversion coefficients β_{lm} become independent of n, and thus the notation β_{lm} is justified. This also reduces the computational task, since then it is necessary to carry out only one inversion for each value of l.

6 ARTIFICIAL DATA

An artificial data set was created for a numerical experiment. The computation was carried out using the full equation (2.1) for the assumed angular velocity $\Omega(r,\mu)$. The data set contains 69 242 p-modes with 1232 distinct (nl) having $5 \le l \le 250$. Gaussian random errors with standard deviation of 3 per cent were added to $\Delta\omega_{nlm}/m$.

7 RESULTS

Fig. 1 shows angular averaging kernels $W_l(\mu,\mu_0)$ for various values of l at three colatitudes ($\theta = 0°, 30°, 90°$), obtained by angular inversion with $\lambda = 10^{-7}$. For low-degree modes, for which there are only few values of m, the averaging kernels are not well localized. With increasing l, the localization improves, but wiggles of small amplitude remain. By increasing λ, however, the amplitude of the wiggles can be made to decrease more rapidly.

In Fig. 2, inversion coefficients $\beta_{lm}(\mu_0)$ for $l = 200$, $\mu_0 = 0.5$ are plotted against m/l. The inversion coefficients are positive on the left-hand side of $m/l \simeq \sqrt{1-\mu_0^2}$, while they are negative on the right-hand side. From this it is apparent that the current inversion is essentially a subtractive operation: from a weighted average of frequency splittings of low-m modes (which penetrate to higher latitudes), a similar average of high-m modes (which penetrate only to lower latitudes) is subtracted to obtain the contribution from the target area. This property is consistent with the asymptotic representation of the frequency splitting, which averages $\Omega(\mu)$ with an Abel kernel and whose inverse is the derivative, with respect to m, of a weighted integral of the splitting (Gough 1990).

Fig. 3 shows the averaging kernel obtained from the modified radial inversion described in Section 4, with $\alpha = 10^4$, for $r_0 = 0.8$, $\theta_0 = 30°$. Here, the full expression for the averaging kernel,

$$D(r,\mu;r_0,\mu_0) = \sum_{nlm} c_{nl}\beta_{lm}\left[K_{nl}(r)W_{lm}(\mu) + L_{nl}(r)X_{lm}(\mu)\right] \ , \tag{7.1}$$

has been used; the coefficients c_{nl} have been scaled by a constant to render the averaging kernel unimodular.

The averaging kernel is well localized near the target point. The radial inversion coefficients c_{nl} are shown in Fig. 4. In contrast to Fig. 2, the inversion is not a simple subtractive operation. This result is consistent with what Christensen-Dalsgaard, Schou & Thompson (1990) reported on the standard one-dimensional optimal averaging.

For a comparison, I replaced the coefficients c_{nl} in equation (7.1) by coefficients c^*_{nl} which were obtained from the standard one-dimensional optimal averaging (cf. equation 3.3). The parameter for the inversion was adjusted to produce a comparable result to the one shown in Fig. 3. The averaging kernel thus produced is shown in Fig. 5; once again, the kernel has been scaled to be unimodular.

Note that in this case the l-dependence of the angular averaging kernel is rather weak, at least for high degree (Fig. 1). Nevertheless, the distortion of the averaging kernel is significant, as was discussed in Section 3. Between the centre of the kernel and the surface of the star is a structure which includes both positive and negative contributions. If $\Omega(r,\mu)$ were very smooth, one could hope that these opposing contributions largely cancel. However, since we do not know whether Ω is smooth, the existence of this structure makes

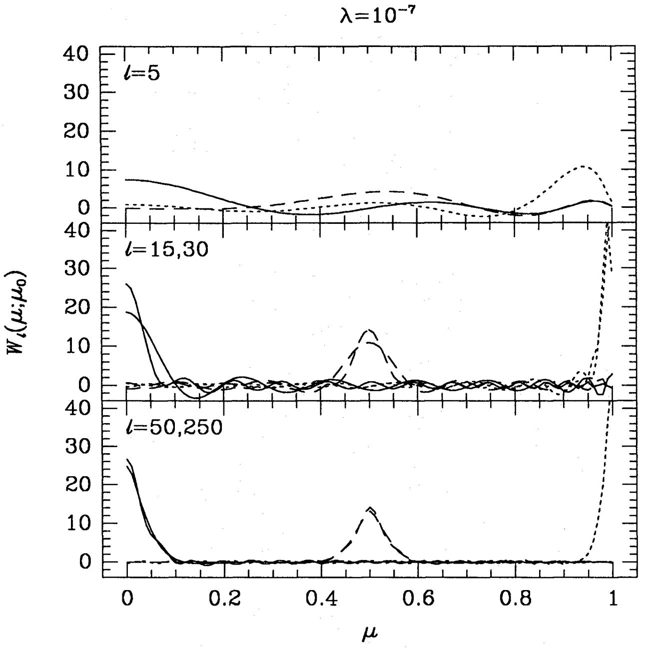

Figure 1. Angular averaging kernels W_l for various values of l at $\theta_0 = 0°$(solid lines), $\theta_0 = 30°$(short-dashed lines) and $\theta_0 = 90°$(long-dashed lines). In the central panel the narrower kernels were produced from the modes with the higher value of l. The same is true also in the bottom panel, though in that case the differences are barely discernible.

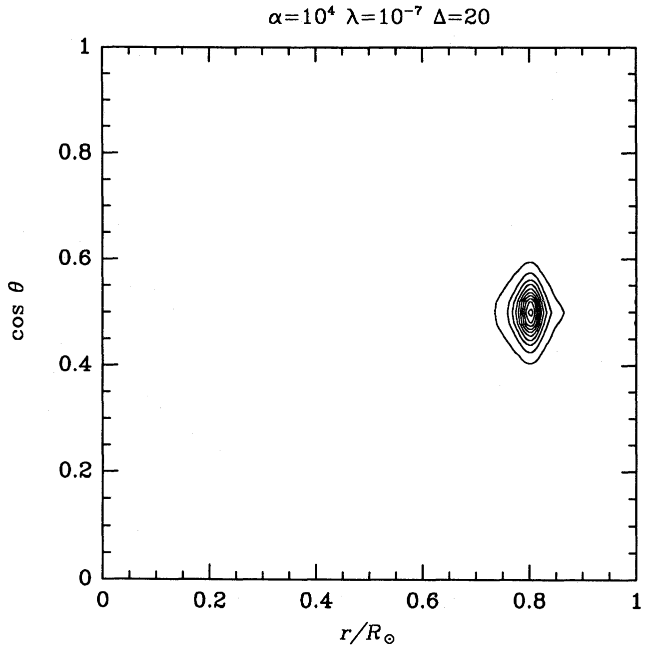

Figure 3. Contour map of the full averaging kernel with $r_0 = 0.8$, $\theta_0 = 30°$, $\alpha = 10^4$ and $\lambda = 10^{-7}$. The contours are separated by an interval of 20 and range from −10 to 190. The contour representing the negative value exists only in a very thin surface layer and is visible in the figure.

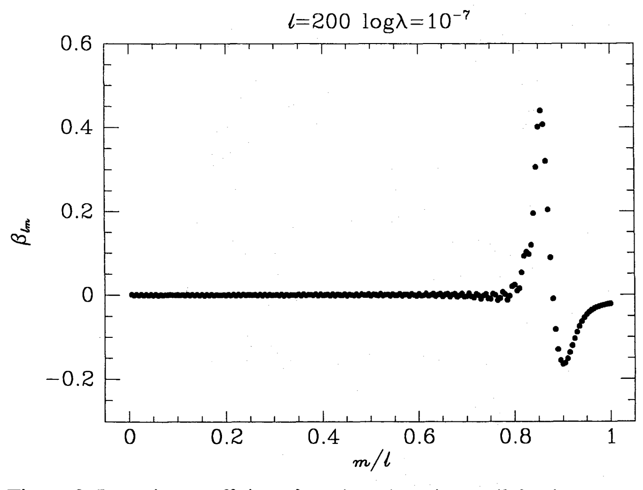

Figure 2. Inversion coefficient β_{lm} plotted against m/l for $l = 200$ at $\theta_0 = 30°$.

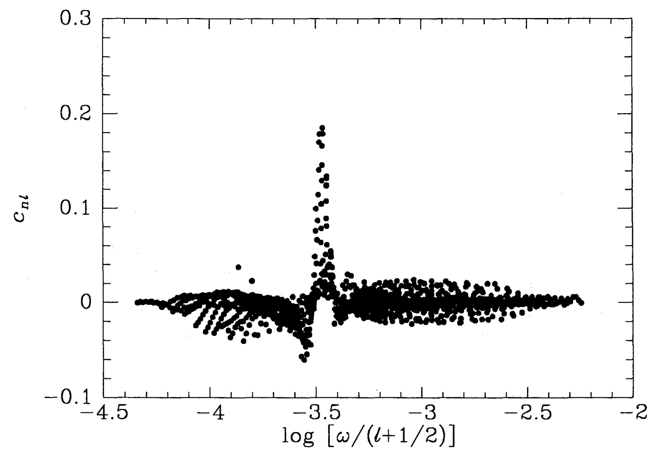

Figure 4. Inversion coefficient c_{nl} for the averaging kernel in Fig. 3, plotted against $\log[\omega_{nl0}/(l+1/2)]$.

it difficult to interpret what we obtain as an estimate of the angular velocity at the target point. Therefore the straightforward $R^1 \otimes R^1$ inversion technique is evidently inferior to the modified procedure described in Section 4, whose averaging kernel is depicted in Fig. 3.

For another comparison, the approximate averaging kernel obtained by ignoring the second term in square brackets in the expression (7.1) is shown in Fig. 6. The difference between the approximate kernel and the full kernel (Fig. 3) is visible, but the contribution from the extra term $L_{nl}(r)X_{lm}(\mu)$, which is present in the full kernel, is mostly confined to the central peak and thus does not deform the averaging kernel in an undesirable way.

With the same λ and α, the radial resolution becomes poorer with increasing depth because of the relative sparseness of modes in the deep interior. The radial resolution also changes with colatitude, because of the term that accounts for error magnification in expression (4.2). Details of the result would be different for different distributions of e_{nlm}, but the overall behaviour of the variation of the radial resolution is robust.

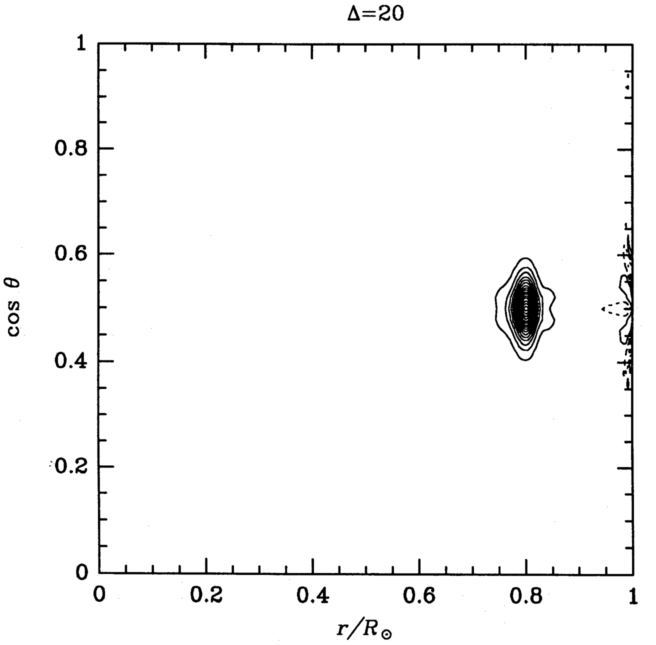

Figure 5. Averaging kernel obtained by using the simple radial optimal averaging. The spacing of the contours is the same as in Fig. 3. Dashed contours represent negative values.

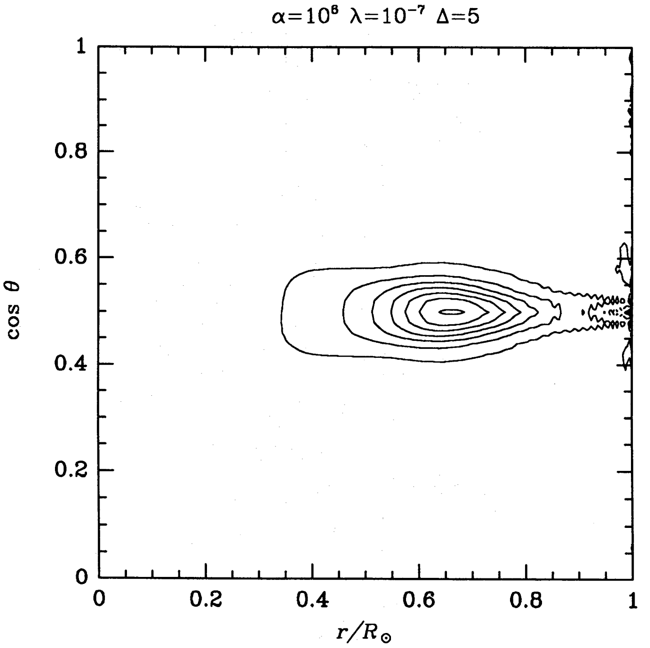

Figure 7. Contour map of the full unimodular averaging kernel with $r_0 = 0.6$, $\theta_0 = 30°$, $\alpha = 10^6$ and $\lambda = 10^{-7}$. The spacing of the contours is 5. Dashed contours represent negative values.

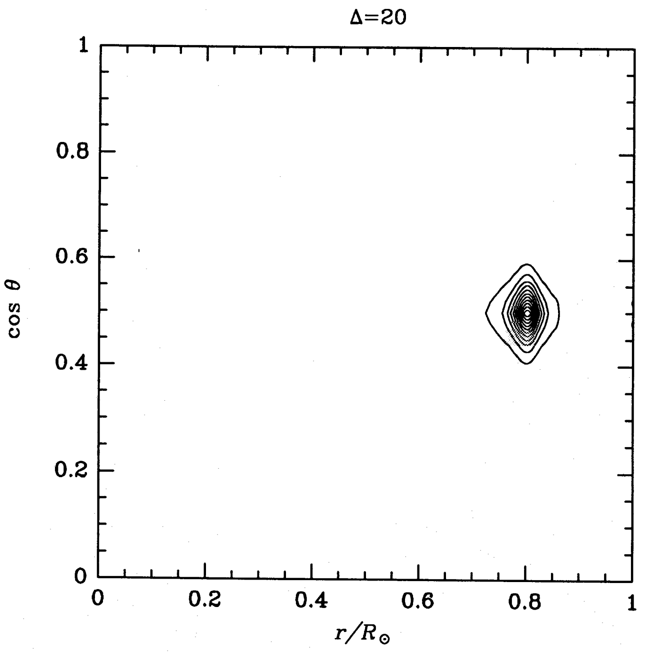

Figure 6. Averaging kernel obtained from the approximation to expression (7.1) obtained by ignoring the small second term. The spacing of the contours is the same as in Fig. 3.

In the deeper layers, the result for high angular resolution is often poor, even with low radial resolution (Fig. 7). This is because for lower degree modes, which are important in the deeper layers, the l-dependence of W_l is stronger. Better results are obtained for high radial resolution with low angular resolution (Fig. 8): higher radial resolution demands weaker l-dependence of W_l, which is realized with lower angular resolution.

8 DISCUSSION

The simplest $R^1 \otimes R^1$ inversion does not produce 'good' averaging kernels, even if the l-dependence of the angular averaging kernels is fairly weak. It has been shown, however, that a simple modification to the radial inversion produces well-localized averaging kernels with less severe sidelobes.

This work suggests that it is difficult to use any method other than optimal averaging for radial inversion. One might work harder to obtain less l-dependent angular averaging kernels. The subtractive optimally localized average, suggested by Pijpers & Thompson (1992), could be tried for this purpose. The example shown above suggests that the l-dependence must be very weak for us to be able to ignore it. Even if one is going to use the modified algorithm described in Section 4, the weak dependence on l of the angular averaging kernel is desirable, and thus the potential application of the technique is certainly interesting.

Another modification to the original $R^1 \otimes R^1$ strategy is to carry out more than one set of angular inversions; we should choose an angular resolution appropriate to the target depth. Angular resolution is determined mainly by the degree of those modes that are the main contributors to the averaging kernel, and that in turn depends on the target depth. It is not necessary to carry out a separate angular inversion for each radial mesh point, however; in practice it is sufficient to carry out only a few sets of angular inversions to cover the whole range of depths.

The current method can be interpreted as an approximate version of 2D optimal averaging. In 2D optimal averaging we would obtain each c_{nlm} independently. Here, the coefficients have been factored in the form $c_{nlm} = c_{nl}\beta_{lm}$, which reduces the computational burden dramatically. A drawback is that now one has less freedom to choose c_{nlm}, and therefore the

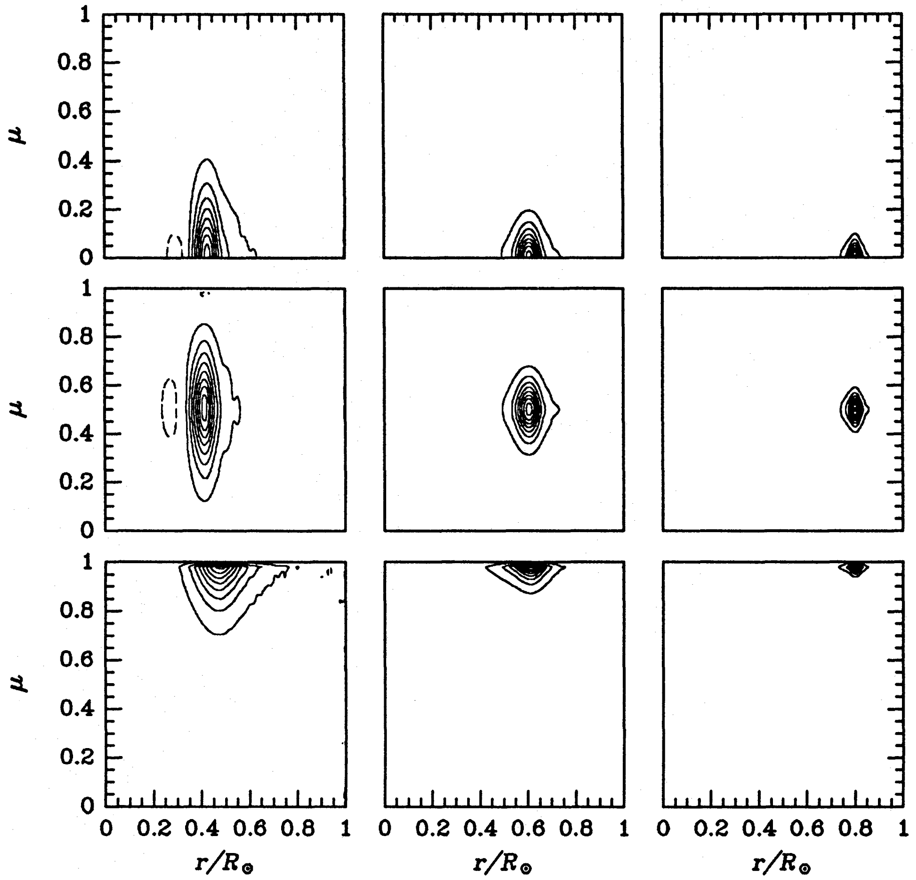

Figure 8. Contour maps of full unimodular averaging kernels for $\theta_0 = 90°$ (top row), $\theta_0 = 30°$ (middle row) and $\theta_0 = 0°$ (bottom row); $r_0 = 0.4$ (left column), $r_0 = 0.6$ (middle column) and $r_0 = 0.8$ (right column). The inversion parameters are $\alpha = 10^2$, $\lambda = 10^{-5}$ ($r_0 = 0.4$), $\alpha = 10^4$, $\lambda = 10^{-6}$ ($r_0 = 0.6$) and $\alpha = 10^4$, $\lambda = 10^{-7}$ ($r_0 = 0.8$). The spacing of the contours is 1/8 of the heights (above zero) of the peaks of the averaging kernels. Dashed contours represent negative values.

averaging kernel is not as good as it might have been.

Another fundamental drawback to the current algorithm is the difficulty in treating low-degree modes. A possible way to remove this symptom is to stop using β_{lm} for low-degree modes. The full set of parameters c_{nlm} can be adopted for the modes of low degree, and the factorized form only for the modes of higher degree. While special care should be given to angular localization, this hybrid procedure hardly increases the number of adjustable parameters that need to be found. However, it is not guaranteed that inclusion of lower degree modes improves the result in the deep interior significantly. Strong angular localization is not possible because there are only a few distinct singlets when l is small.

Finally, it is noted that the separation of radial and angular inversions is possible even if the term $G_{nl}X_{lm}$ in equation (2.1) is retained. For example, the regularized least-squares data fitting could be used to fit both F_{nl} and G_{nl} simultaneously for each value of l. Subsequently, these results should be merged in some way and inverted in the radial direction, because both F_{nl} and G_{nl} are weighted averages of $\Omega(r, \mu)$. Thus the procedure would be quite complicated, and without specifying the detail it is not obvious whether a modified radial inversion procedure parallel to the one proposed in this paper can be developed. This procedure would also aggravate the difficulty for the low-degree modes, because then one is trying to extract even more information from a small number of singlets.

ACKNOWLEDGMENTS

The author thanks D.O. Gough and A.G. Kosovichev for useful discussion and encouragement. He is grateful to the SERC for financial support.

REFERENCES

Backus G., Gilbert F., 1968, Geophys. J., 16, 169

Backus G., Gilbert F., 1970, Phil. Trans. R. Soc. Lond. A, 266, 123

Brown T. M., Christensen-Dalsgaard J., Dziembowski W. A., Goode P., Gough D. O., Morrow C. A., 1989, ApJ, 343, 526

Christensen-Dalsgaard J., Schou J., Thompson M. J., 1990, MNRAS, 242, 353

Duvall T. L., Jr, Harvey J. W., 1984, Nat, 310, 19

Duvall T. L., Jr, Dziembowski W. A., Goode P. R., Gough D. O., Harvey J. W., Leibacher J. W., 1984, Nat, 310, 22

Gough D. O., 1984, Phil. Trans. R. Soc. Lond. A, 313, 27

Gough D., 1985, Sol. Phys., 100, 65

Gough D. O., 1990, in Osaki Y., Shibahashi H., eds, Progress of Seismology of the Sun and Stars. Springer-Verlag, Berlin, p.283

Gough D. O., Toomre J., 1991, ARA&A, 29, 627

Hansen C. J., Cox J. P., Van Horn H. M., 1977, ApJ, 217, 151

Harvey J. W., Hill F., Kennedy J. R., Leibacher J. W., 1993, in Brown T. M., ed., ASP Conf. Ser. Vol. 42, GONG 1992: Seismic Investigation of the Sun and Stars. Astron. Soc. Pac., San Francisco, p.397
Phillips D. L., 1962, J. Assoc. Comput. Mach., 9, 84
Pijpers F. P., Thompson M. J., 1992, A&A, 262, L33
Scherrer P. H. et al., 1989, in Domingo V., ed., The SOHO Mission. ESA SP-1104, Noordwijk, p.25
Schou J., 1991, in Gough D. O., Toomre J., eds, Challenges to Theories of the Structure of Moderate-Mass Stars. Springer-Verlag, Berlin, p.93
Schou J., Christensen-Dalsgaard J., Thompson M. J., 1993a, in Baglin A., Weiss W. W., eds, Proc. IAU Colloq. 137, Inside the Stars. Astron. Soc. Pac., San Francisco, p72.
Schou J., Christensen-Dalsgaard J., Thompson M. J., 1993b, in Brown T. M., ed., ASP Conf. Ser. Vol. 42, GONG 1992: Seismic Investigation of the Sun and Stars. Astron. Soc. Pac., San Francisco, p.205
Sekii T., 1990, in Osaki Y., Shibahashi H., eds, Progress of Seismology of the Sun and Stars. Springer-Verlag, Berlin, p.337
Sekii T., 1991, PASJ, 43, 381
Sekii T., 1993, in Brown T. M., ed., ASP Conf. Ser. Vol. 42, GONG 1992: Seismic Investigation of the Sun and Stars. Astron. Soc. Pac., San Francisco, p.237
Tikhonov A. N., 1963, Sov. Maths-Dokl., 4, 1035
Twomey S., 1963, J. Assoc. Comput. Mach., 10, 97
Unno W., Osaki Y., Ando H., Saio H., Shibahashi H., 1989, Nonradial Oscillations of Stars. Univ. Tokyo Press, Tokyo

This paper has been produced using the Blackwell Scientific Publications TEX macros.